Self-assembly of a functional oligo(aniline)-based amphiphile into helical conductive nanowires

O. Alexander Bell,[a] Guanglu Wu,[b] Johannes S. Haataja,[c] Felicitas Brömmel,[a] Natalie Fey,[a] Annela M. Seddon,[d, e] Robert L. Harniman,[a] Robert M. Richardson,[d] Olli Ikkala,[c] Xi Zhang,[b] Charl FJ Faul*[a]

Supporting information

Table of Contents

Materials and methods

Instrumentation

High-resolution mass spectrometry was performed using either Bruker Daltronics UltrafleXtreme (MALDI-TOF) or MicrOTOF II (ESI-TOF) mass spectrometers. ^{1}H and ^{13}C NMR experiments were performed using either a 400 MHz Varian VNMR 400, a 500 MHz Bruker 500 NMR spectrometer with CryoProbe or a 500 MHz Varian VNMRS500 for 2D NOESY experiments, and referenced to deuterated solvents. UV/Vis experiments were performed using a Shimadzu UV 2600 spectrophotometer with integrating sphere attachment. Spectra were recorded using a 1mm path length quartz cuvette due to strong absorbance of the samples. Temperature-dependent UV/Vis experiments were performed on a Perkin-Elmer Lambda 35 spectrophotometer with a Peltier temperature controller, using 1 mM aqueous solutions and a 1 mm quartz cuvette. Spectra of solvent baselines were subtracted from the data. Circular dichroism and linear dichroism spectra were recorded using a Jasco J-810 spectropolarimeter.

For CD, a quartz sandwich cell with an approximate pathlength of 0.1 mm was used due to the high intensity of absorbance of the samples. For LD, a micro-volume quartz Couette flow cell with annular path length of 0.25 mm. was used. CD and LD spectra were recorded in Milli-Q ultrapure deionised water. LD spectra were processed by subtraction of non-rotating baseline spectra. All spectra were obtained at room temperature unless otherwise stated. Fluorescence spectra were obtained using a Hitachi F-7000 spectrofluorometer, using a cuvette with 1 cm path length, with the temperature controlled at 25 °C for all experiments. 10 μL of a 0.5 mg/mL pyrene solution in acetone was added to 900 μL EB TANI-PTAB aqueous solutions with different concentrations. After sonicating for 10 min, the pyrene emission band (between 360 and 450 nm excited at 337 nm) of each solution was recorded. The CMC was chosen as the concentration where the pyrene exhibited an apparent decrease in the I_{373nm}/I_{383nm} ratio (denoted as I_1/I_3) with increasing concentration.

Atomic force microscopy was performed using either a Bruker Multimode 8 AFM with a Nanoscope V controller and PeakForce feedback or a Bruker Multimode AFM with a Nanoscope III controller in tapping-mode. Samples were drop-cast onto freshly cleaved HOPG surfaces and excess solution was wicked off using filter paper. Images were recorded after drying the sample in ambient conditions and processed using Bruker Nanoscope Analysis software.

Transmission electron microscopy images were recorded using a JEOL 1200 TEM MK2 with a tungsten filament, operated at a frequency of 120 kV and equipped with MegaView II digital camera using Soft Imaging Systems 3.0 image software. Samples were drop-cast onto Formvar-coated 150 mesh copper grids and blotted with filter paper before drying in air. Uranyl acetate (1%, aq.) was then applied and blotted with filter paper after 30s, then the sample allowed to dry in ambient conditions. Cryo-transmission electron microscopy (cryo-TEM) imaging was carried out using a JEOL JEM 3200FSC field emission microscope operated at 300 kV in bright field mode with Omega-type Zero-loss energy filter. The images were acquired with Ultrascan 4000 CCD camera (Gatan) and with Gatan Digital Micrograph software (version 1.83.842), while the specimen temperature was maintained at -187 °C. Vitrified samples were prepared using FEI Vitribot placing a 3 μL sample solution on 200 mesh lacey carbon copper grids under 100% humidity, then blotted with filter paper 0.5–1.5 s and immediately plunged to -170 °C ethane/propane mixture and cryotransferred to the microscope.

X-ray scattering data were collected on a Ganesha SAXS/WAXS instrument (SAXSLAB) at room temperature over a Q-range of $0.001< Q <0.7$ Å^{-1}. Samples were loaded into quartz capillaries (Gulmay Scientific) and sealed with epoxy. Data were collected over an exposure time of 3 hours and background-corrected with water. Data analysis was performed using SASFit.

Polarising optical microscopy images were collected using an Olympus BX50 microscope fitted with an Olympus C-5060 digital camera.

Conductivity measurements were made using a custom-built 4-point probe station with a Keithley 2401 low voltage sourcemeter. Substrates were prepared by sputtering 50 nm thick gold electrodes in a collinear 4-point probe configuration onto a quartz substrate through a custom-made mask. Electrode separations were 0.25mm. Films were spin-coated onto these electrode-bearing quartz substrates, and film thickness was measured after resistance measurements by scratching the film and imaging using AFM. CSA-doped solutions were prepared by dissolving solid EB TANI-PTAB of the required mass in ultrapure deionised water with the aid of ultrasonication and vortex mixing, followed by adjustment to the correct concentration and acid doping by addition of the required volume of a given concentration of CSA in aqueous solution to achieve a 2:1 acid: TANI-PTAB molar ratio in solution.

Reagents

Reagents were purchased from Sigma-Aldrich UK and used as received. Molecular sieves were activated by heating at 200 °C under dynamic vacuum overnight. Solvents were anhydrous unless specified otherwise.

Synthesis of EB TANI-PTAB

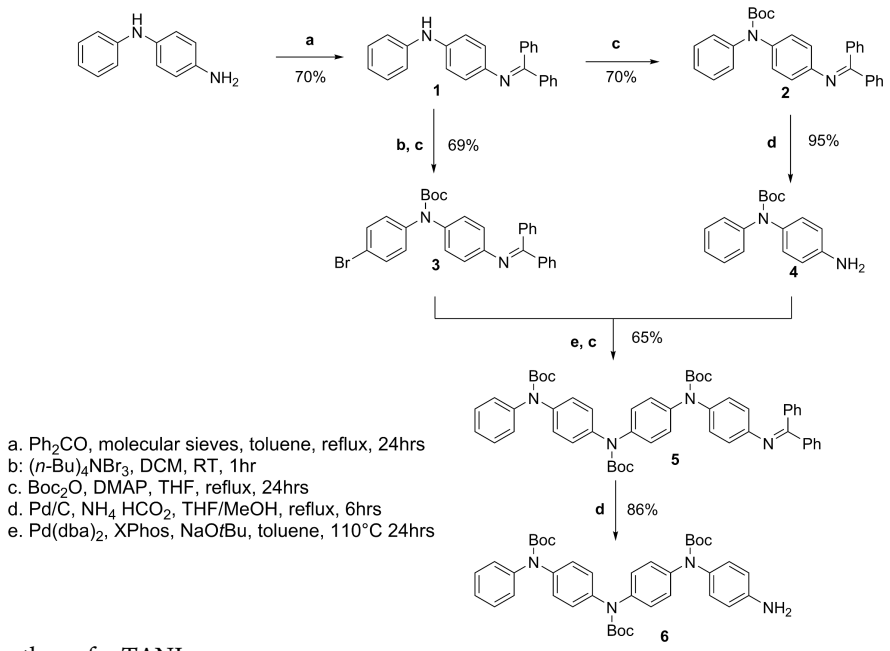

Scheme S1 – Synthesis pathway for TANI precursor

Synthesis of TANI precursor

4-((diphenylmethylene)amino)-N-phenylaniline (1)

Activated molecular sieves (100 g, 3Å) were added to a solution of *N*-phenyl-*p*-phenylene diamine (1.05 eq, 27.65 g, 150 mmol) and benzophenone (1 eq, 25g, 135 mmol) in toluene (150 mL) under nitrogen atmosphere. The mixture was refluxed for 24 hours and a strong yellow colour developed. The sieves were removed, washed with THF and combined with the toluene mixture. The solvent was removed to give a brown oil that solidified into a bright yellow solid when methanol (100 mL) was added. The suspension was filtered and the filtrate concentrated, and filtered again. The combined solids were recrystallized from methanol to yield yellow crystals; with concentration of the mother liquor yielding a second crop (70 % yield).

^{1}H NMR (500 MHz, DMSO-d_6) δ 7.97 (s, 1H), 7.64 (d, J = 6.8 Hz, 2H), 7.49 (t, 1H), 7.44 (t, J = 7.5 Hz, 2H), 7.40 – 7.31 (m, 3H), 7.21 – 7.11 (m, 4H), 6.94 (d, J = 7.3 Hz, 2H), 6.86 (d, J = 8.6 Hz, 2H), 6.75 (t, J = 7.3 Hz, 1H), 6.60 (d, J = 8.6 Hz, 2H). ^{13}C NMR (126 MHz, DMSO-d_6) δ 144.28 , 144.02 , 139.44 , 136.89 , 131.06 , 129.57 , 129.39 , 129.03 , 128.91 , 128.75 , 128.67 , 122.59 , 119.55 , 117.80 , 116.45 .

HRMS: $[M+H]^+$ = 349.1709 (Calculated for $C_{25}H_{21}N_2$ = 349.1699) (ESI-TOF)

tert-butyl (4-((diphenylmethylene)amino)phenyl)(phenyl)carbamate (2)

To a solution of **1** (1 eq.) in THF under a nitrogen atmosphere was added *di-tert*-butyl dicarbonate (1.2 eq.) and dimethylaminopyridine (0.1 eq.). The solution was refluxed for 24hrs, after which time the mixture was allowed to cool to room temperature and ethanol (2x volume of THF) was added. The mixture was cooled in the fridge overnight and filtered, yielding fine pale-yellow needles. Concentration of the filtrate yielded a second crop of crystals (78% yield).

^{1}H NMR (500 MHz, Chloroform-d) δ 7.77 (d, J = 7.0 Hz, 1H), 7.49 (t, J = 7.3 Hz, 1H), 7.43 (t, J = 7.5 Hz, 2H), 7.35 – 7.24 (m, 5H), 7.20 – 7.10 (m, 5H), 7.00 (d, J = 8.6 Hz, 2H), 6.70 (d, J = 8.6 Hz, 2H), 1.42 (s, 9H). ^{13}C NMR (126 MHz, Chloroform-d) δ 168.68 , 153.85 , 149.06 , 143.14 , 139.54 , 138.31 , 136.13 , 130.81 , 129.55 , 129.33 , 128.66 , 128.51 , 128.22 , 127.92 , 127.46 , 126.19 , 125.11 , 121.37 , 80.88 , 77.23 , 28.23

HRMS: $[M]^+$ = 449.2223 (Calculated for $C_{30}H_{29}N_2O_2$: 449.2224) (MALDI-TOF)

tert-butyl (4-bromophenyl)(4-((diphenylmethylene)amino)phenyl)carbamate (3)

To a solution of **2** (1 eq, 500 mg, 1.11 mmol) in dichloromethane (10 mL) was added tetrabutylammonium tribromide (1.1 eq.) in one shot. The mixture was stirred at room temperature for 1 hour before sodium sulfite (aq., 22%, 5 mL) was added. The mixture was stirred a further 30 minutes at room temperature before sodium hydroxide (2 M, 5 mL) was added with stirring. The mixture was then separated and the organic phase washed with deionised water (3 x 20 mL) followed by drying over anhydrous $MgSO_4$. The solvent was evaporated and di-*tert*-butyl dicarbonate (1.1 eq) and dimethylaminopyridine (0.1 eq) were added to the residue. The mixture was taken up in THF (100 mL)

and refluxed overnight. After cooling to room temperature, ethanol (200 mL) was added and the mixture was cooled in the fridge. Filtration, followed by concentration of the mother liquor to recover a second crop yielded the product as fine pale-yellow needles (69 % yield).
1H NMR (500 MHz, DMSO-d6) δ 7.68 – 7.64 (m, 2H), 7.56 – 7.50 (m, 1H), 7.50 – 7.44 (m, 4H), 7.34 – 7.28 (m, 3H), 7.17 – 7.10 (m, 2H), 7.08 (d, J = 8.8 Hz, 2H), 6.98 (d, J = 8.6 Hz, 2H), 6.67 (d, J = 8.6 Hz, 2H), 1.31 (s, 9H). ^{13}C NMR (126 MHz, DMSO-d6) δ 168.50 , 149.85 , 142.73 , 139.08 , 137.70 , 131.92 , 131.51 , 129.31 , 129.25 , 129.05 , 128.86 , 128.47 , 128.07 , 121.35 , 118.03 , 80.96 , 28.23 .
HRMS: $[M]^+$ = 527.1324 (Calculated for $C_{30}H_{28}BrN_2O_2$: 527.1329) (MALDI-TOF)

tert-butyl (4-aminophenyl)(phenyl)carbamate (4)

To a solution of **3** (1 g, 2.23 mmol, 1 eq) in a THF-methanol mixture (1:2.5, respectively) was added ammonium formate (12 eq., 1.68 g, 26.8 mmol) and palladium on carbon (10 % Pd by weight, 2.5 mol% Pd vs. 3, 60 mg) under a nitrogen atmosphere. The mixture was refluxed for 24 hours, after which time completion was confirmed by TLC (1:1 ethyl acetate:n-hexane). The reaction was cooled to room temperature and the solvent removed. The residue was taken up in dichloromethane (50 mL) and filtered through a plug of celite. The celite was washed with DCM and the filtrate evaporated. The residue was stirred in n-hexane (150 mL) for 1 hour followed by filtration and washing with hexane to yield the product as an off-white powder (96 % yield).
1H NMR (500 MHz, DMSO-d6) δ 7.28 (t, J = 7.8 Hz, 2H), 7.16 (d, J = 7.4 Hz, 2H), 7.12 (td, J = 7.2, 1.2 Hz, 1H), 6.84 (d, J = 8.6 Hz, 2H), 6.50 (d, J = 8.6 Hz, 2H), 5.09 (s, 2H), 1.35 (s, 9H). ^{13}C NMR (126 MHz, DMSO-d6) δ 153.93 , 147.49 , 144.12 , 131.73 , 128.91 , 128.71 , 126.61 , 125.36 , 114.27 , 80.11 , 39.73 , 28.38 .
HRMS: $[M+Na]^+$: = 307.1411 (Calculated for $C_{17}H_{20}N_2O_2Na$: 307.1417) (MALDI-TOF)

tert-butyl (4-((tert-butoxycarbonyl)(4-((tert-butoxycarbonyl)(4-((diphenylmethylene)amino)phenyl)amino)phenyl)amino)phenyl)(phenyl)carbamate (5)

To a pre-dried Young's tap Schlenk tube was added **3** (5g, 9.48 mmol, 1eq), **4** (3.23 g, 11.4 mmol, 1.2 eq), $Pd(dba)_2$ (100 mg, 2 mol%), XPhos (90 mg, 2 mol%) and sodium *tert*-butoxide (1.82 g, 2eq). The reagents were protected under nitrogen and toluene (anhydrous, 100 mL) was added. The tube was sealed and heated at 110°C for 2 days, until complete consumption of **4** was observed by TLC. The reaction was allowed to cool to room temperature and filtered through celite, then all solvent removed. The residue was taken up in dichloromethane and washed with deionised water, followed by drying of the organic phase over $MgSO_4$ and evaporation of the solvent. To the residue were added di-*tert*-butyl dicarbonate (1.3 eq) and dimethylaminopyridine (0.1 eq) and THF (100 mL), and the mixture was refluxed under nitrogen for 3 days. When complete, the solvent was removed and the residue washed with methanol and filtered to give the product as a pink-beige powder (65% yield).
^{1}H NMR (500 MHz, Chloroform-d) δ 7.77 – 7.71 (m, 2H), 7.50 – 7.45 (m, 1H), 7.40 (dd, J = 8.2, 6.8 Hz, 2H), 7.34 – 7.22 (m, 5H), 7.21 – 7.04 (m, 13H), 6.98 – 6.92 (m, 2H), 6.70 – 6.63 (m, 2H), 1.43 (d, J = 5.6 Hz, 18H), 1.38 (s, 9H).^{13}C NMR (126 MHz, Chloroform-d) δ 153.75 , 149.19 , 140.39 , 140.10 , 139.51 , 138.00 , 130.82 , 129.52 , 129.33 , 128.73 , 128.69 , 128.22 , 127.92 , 127.49 , 127.01 , 126.96 , 126.91 , 126.14 , 125.74 , 121.39 , 81.31 , 81.25 , 81.01 , 28.23 , 28.21 .
HRMS: $[M+H]^+$ = 831.4111 (Calculated for $C_{52}H_{55}N_4O_6$: 831.4116)

tert-butyl (4-aminophenyl)(4-((tert-butoxycarbonyl)(4-((tert-butoxycarbonyl)(phenyl)amino)phenyl)amino)phenyl)carbamate (6)

To a flask was added **5** (1eq), Pd/C (10% Pd content, 2mol%) and ammonium formate (10 eq). THF and methanol were added (in a ratio of 1:2.5, respectively) and the suspension was refluxed under nitrogen until TLC (1:1 ethyl acetate:n-hexane) confirmed completion (24hrs). The solvent was removed and the taken up in DCM, then filtered through celite and washed with DCM. The filtrate was evaporated and the residue stirred in hexane for 1 hour, followed by 1 hr. sonication, and then filtered to obtain the product as an off-white powder (86% yield).
1H NMR (500 MHz, DMSO-d6) δ 7.34 (t, J = 7.8 Hz, 2H), 7.20 (dd, J = 8.4, 7.1 Hz, 3H), 7.17 – 7.07 (m, 8H), 6.86 – 6.80 (m, 2H), 6.53 – 6.46 (m, 2H), 5.10 (s, 2H), 1.38 – 1.32 (m, 27H). 13C NMR (126 MHz, DMSO-d6) δ 153.34 , 147.61 , 143.07 , 140.67 , 131.42 , 129.32 , 128.73 , 127.65 , 127.60 , 127.52 , 127.44 , 126.70 , 126.37 , 114.31 , 80.96 , 80.94 , 80.24 , 28.34 , 28.25 .
HRMS: $[M+K]^+$ 705.3044 (calculated for $C_{39}H_{46}N_4O_6K$: 705.30489

Synthesis of TANI-PTAB

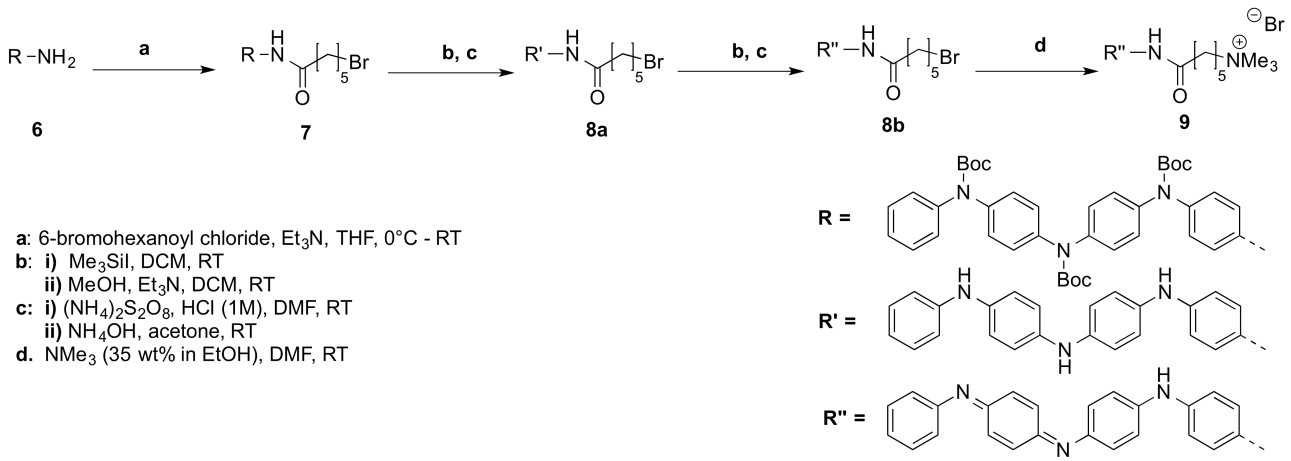

Scheme S2 - Synthesis of EB TANI-PTAB

tert-butyl (4-(6-bromohexanamido)phenyl)(4-((tert-butoxycarbonyl)(4-((tert-butoxycarbonyl)(phenyl)amino)phenyl)amino)phenyl)carbamate (7)

To an ice-cooled solution of **6** (500 mg, 0.75 mmol, 1 eq) in THF (anhydrous, 50 mL) in a flask under a nitrogen atmosphere and equipped with a dropping funnel was added triethylamine (5 eq, 380 mg). To this mixture was added dropwise a solution of 6-bromohexanoyl chloride (1.05 eq, 168 mg) in THF (10 mL) with stirring and ice cooling. Once addition was complete, the ice bath was removed and the solution allowed to warm up to room temperature. After TLC (1:1 ethyl acetate: n-hexane) confirmed consumption of the starting amine, the solvent was removed and the residue taken up in ethyl acetate. The organics were washed with HCl (1 M), NaOH (1 M) and brine before drying over $MgSO_4$ and removing the solvent to yield the crude product as an off-white solid. This was purified by flash column chromatography (silica gel, 1:1 ethyl acetate:n-hexane) to yield the product as a white solid **7** (80% yield).
^{1}H NMR (500 MHz, DMSO-d_6) δ 9.92 (s, 2H), 7.55 (d, J = 8.8 Hz, 2H), 7.34 (t, 1H), 7.24 – 7.08 (m, 13H), 3.53 (t, J = 6.7 Hz, 2H), 2.30 (t, J = 7.3 Hz, 2H), 1.81 (h, J = 6.9 Hz, 2H), 1.60 (p, J = 7.5 Hz, 2H), 1.41 (p, J = 7.5, 6.9 Hz, 2H), 1.37 (s, 27H). ^{13}C NMR (126 MHz, DMSO-d_6) δ 171.51 , 153.45 , 153.34 , 153.32 , 143.06 , 140.74 , 140.46 , 129.33 , 128.08 , 127.67 , 127.60 , 127.54 , 127.29 , 126.39 , 119.82 , 81.02 , 80.94 , 80.82 , 36.63 , 35.52 , 32.50 , 28.28 , 28.25 , 28.23 , 27.67 , 24.71 .
HRMS: $[M+K]^+$ = 881.2889 (Calculated for $C_{45}H_{55}BrN_4O_7K$: 881.2886)

6-bromo-N-(4-((4-((4-(phenylamino)phenyl)amino)phenyl)amino)phenyl)hexanamide (8a)

To a solution of **7** (400 mg, 0.47 mmol, 1 eq.) in anhydrous dichloromethane (40 mL) under a nitrogen atmosphere was added trimethylsilyliodide (0.34 g, 1.7 mmol, 3.6 eq.) dropwise. The mixture was stirred for 1 hour before anhydrous methanol (approx. 0.5 mL) was added dropwise causing precipitation of a pale solid. Methanol addition was stopped when no further precipitate was produced, and the mixture was stirred for a further 30 minutes. Triethylamine (1 mL) was added causing a pale purple colour to develop. This mixture was stirred for 15 minutes before centrifugation and washing with diethyl ether. After 3 washing and centrifugation steps, the supernatant was discarded and the off-white LEB-state Boc-deprotected solid product **8a** was dried in vacuum overnight, and stored under an inert atmosphere (74% yield).
^{1}H NMR (degassed DMSO, under inert atmosphere): 1H NMR (400 MHz, DMSO-d6) δ 9.61 (s, 1H), 7.75 (s, 1H), 7.67 (s, 1H), 7.62 (s, 1H), 7.38 (d, J = 8.7 Hz, 2H), 7.18 – 7.10 (m, 2H), 7.01 – 6.85 (m, 12H), 6.67 (t, J = 7.3 Hz, 1H), 3.54 (t, J = 6.7 Hz, 2H), 2.25 (t, J = 7.3 Hz, 2H), 1.83 (p, J = 6.9 Hz, 2H), 1.60 (p, J = 7.5 Hz, 2H), 1.41 (p, J = 7.8, 7.4 Hz, 2H).
MS (MALDI) m/z 542.4 $[M]^+$

6-bromo-N-(4-(((1E,4E)-4-((4-(phenylamino)phenyl)imino)cyclohexa-2,5-dien-1-ylidene)amino)phenyl)hexanamide (8b)

The solid product **8a** was used directly for oxidation to the EB state: **8a** (150 mg, 0.28 mmol, 1 eq) was dissolved in DMF (15 mL). A solution of ammonium persulfate (1 eq.) in HCl (1M, aq., 10 mL) was added dropwise with stirring causing a dark green precipitate to develop. The mixture was stirred strongly for 30 minutes, followed by centrifugation to collect the precipitate. The precipitate was washed three times with acetone by centrifugation, and the solid was suspended in acetone (150 mL). Ammonium hydroxide (aq., 2M, 20 mL) was added causing the green mixture to turn dark purple, and the mixture stirred for 15 minutes. The acetone was evaporated under vacuum from the resulting solution leaving an aqueous suspension of a dark blue solid. This was centrifuged and washed extensively with water, followed by drying under vacuum to yield the EB state product **8b** (94 % yield). ^{1}H NMR (500 MHz, DMSO-d_6)

δ 9.96 (s, 1H), 8.46 (s, 1H), 7.86 – 6.61 (m, 17H), 3.55 (t, *J* = 6.7 Hz, 2H), 2.31 (t, *J* = 7.4 Hz, 2H), 1.83 (p, *J* = 6.8 Hz, 2H), 1.62 (p, *J* = 7.4 Hz, 2H), 1.43 (p, *J* = 7.4, 6.6 Hz, 2H). ^{13}C NMR (126 MHz, DMSO-d_6) δ 129.65 , 36.67 , 35.56 , 32.52 , 27.71 , 24.79 .
HRMS: $[M+H]^+$ = 541.1605 (calculated for $C_{30}H_{30}BrN_4O$: 541.1598)

N,N,N-trimethyl-6-oxo-6-((4-((4-(((1E,4E)-4-(phenylimino)cyclohexa-2,5-dien-1-ylidene)amino)phenyl)amino)phenyl)amino)hexan-1-aminium bromide (EB TANI-PTAB) (9)

8b (135 mg, 0.25 mmol, 1 eq.) was dissolved in DMF (5 mL) and trimethylamine (35 wt.% in ethanol, 0.5 mL, >10eq.) was added. The mixture was stirred until TLC analysis showed no starting material (100% ethyl acetate). When complete, the DMF solution was added dropwise to ice-cold diethyl ether (250 mL) and allowed to fully precipitate overnight in the freezer. When complete, the suspension was centrifuged and washed with further diethyl ether to remove residual DMF. The residue was dried in vacuum to remove ether, then dissolved in deionised water (250 mL). These solutions were centrifuged to remove any water-insoluble impurities and the supernatant decanted and lyophilised, to give the product **9** as a fluffy blue solid (94% yield).
^{1}H NMR (500 MHz, Acetonitrile-d3) δ 9.19 (s, 1H), 8.68 (s, 1H), 7.75 (t, J = 8.2 Hz, 1H), 7.45 (dd, J = 26.6, 8.6 Hz, 1H), 7.30 (q, J = 7.5 Hz, 1H), 7.25 – 7.02 (m, 5H), 7.02 – 6.93 (m, 2H), 6.97 – 6.89 (m, 3H), 6.91 – 6.76 (m, 2H), 6.52 – 6.25 (m, 1H), 3.31 (dq, J = 11.8, 7.2, 6.0 Hz, 4H), 3.06 (t, J = 3.5 Hz, 19H), 2.47 (q, J = 7.0 Hz, 2H), 2.40 (q, J = 8.7, 7.2 Hz, 1H), 1.89 – 1.76 (m, 2H), 1.75 (h, J = 7.5 Hz, 4H), 1.44 (dt, J = 13.9, 7.0 Hz, 4H).
Two extra ^{1}H signals were observed: δ 8.89 (s, 0.66H), 7.59 (t, J = 8.4 Hz, 1.3H). These were due to positional isomers of the quinoid ring of EB TANI-PTAB, as confirmed through observation of exchange signals in 2D EXSY NMR experiments (500 MHz, acetonitrile-d3, (below).
^{13}C NMR (126 MHz, DMSO-d6) δ 129.70 , 129.51 , 124.14 , 124.06 , 122.19 , 121.95 , 121.05 , 120.75 , 119.74 , 118.61 , 117.92 , 117.81 , 117.06 , 116.98 , 115.94 , 115.04 , 65.61 , 52.63 , 39.58 , 25.90 , 22.43
HRMS: $[M-Br]^+$ = 520.3057 (calculated for $C_{33}H_{38}N_5O$: 520.3071)

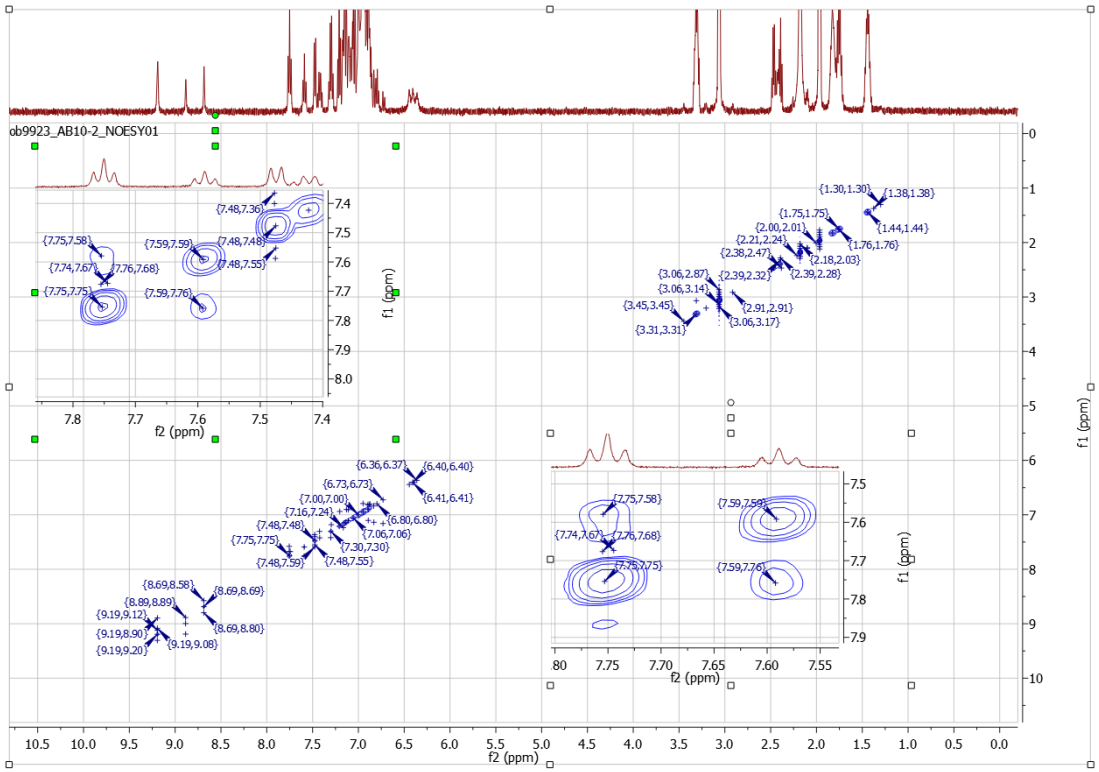

Figure S1. 2D EXSY experiment showing exchange between protons. These exchange signals were excluded from integration to arrive at the correct nuclide count.

Supplementary analysis

For comparison to computationally modelled UV-Vis transitions, the UV/Vis spectrum of EB TANI-PTAB was recorded in acetonitrile, to avoid the affects of self-assembly observed in aqueous solution.

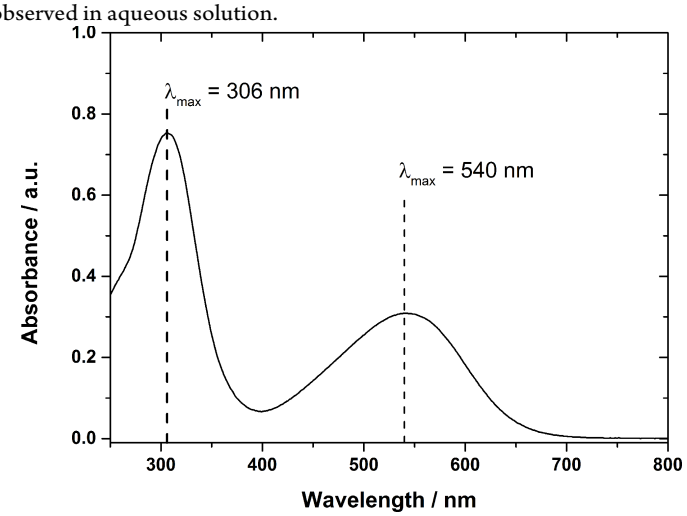

Figure S2 - UV-Vis spectrum of EB TANI-PTAB recorded in acetonitrile

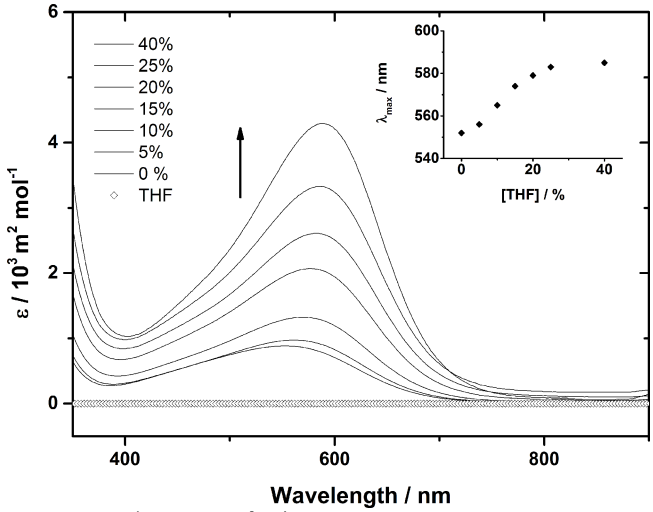

Figure S3. Addition of THF to EB TANI-PTAB (aq., 1×10^{-5} M). Inset: Change of λ_{max} with increasing %THF. Arrow indicates direction of change with increasing [THF]

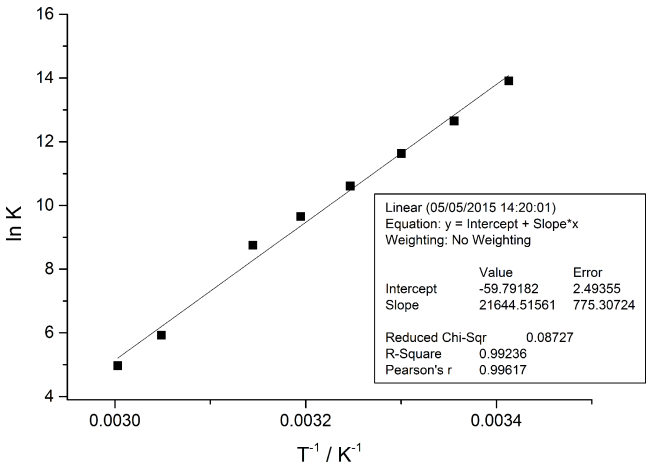

Figure S4 - Van't Hoff plot for EB TANI-PTAB

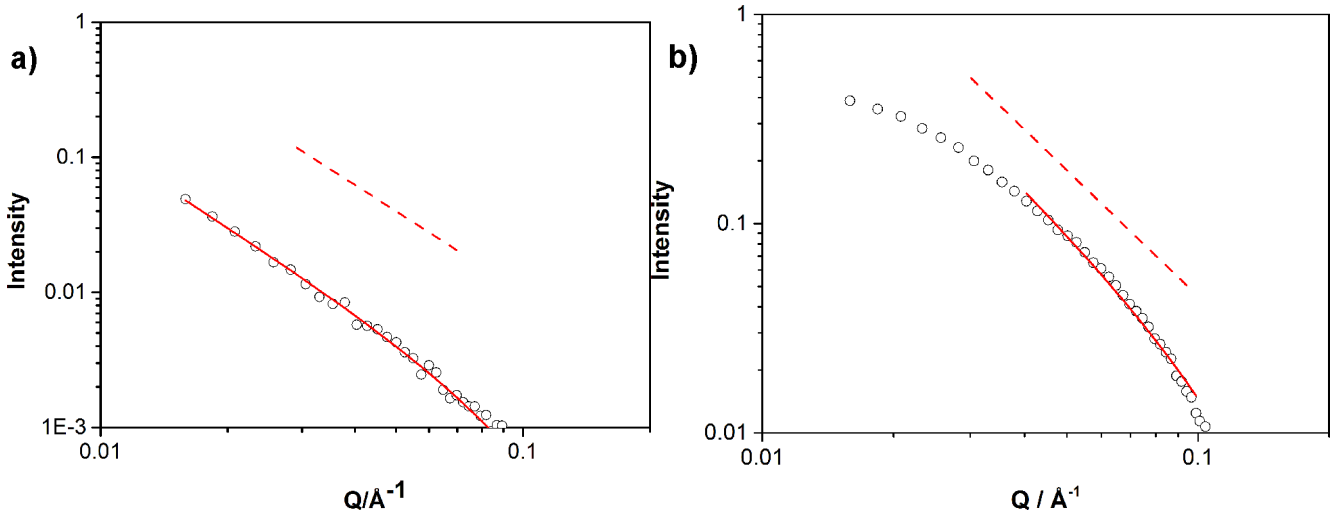

Figure S5. (a) Solution SAXS data for EB TANI-PTAB (4×10^{-3} M) (open circles) with the fit to the thin plate model overlaid (solid red line), thus confirming Q^{-2} dependence (dashed red line). (b) Solution SAXS data for TANI$(CSA)_2$-PTAB (8×10^{-3} M) (open circles) with fit to a thin plate model overlaid (solid red line) and a Q^{-2} dependence indicated (dashed red line)

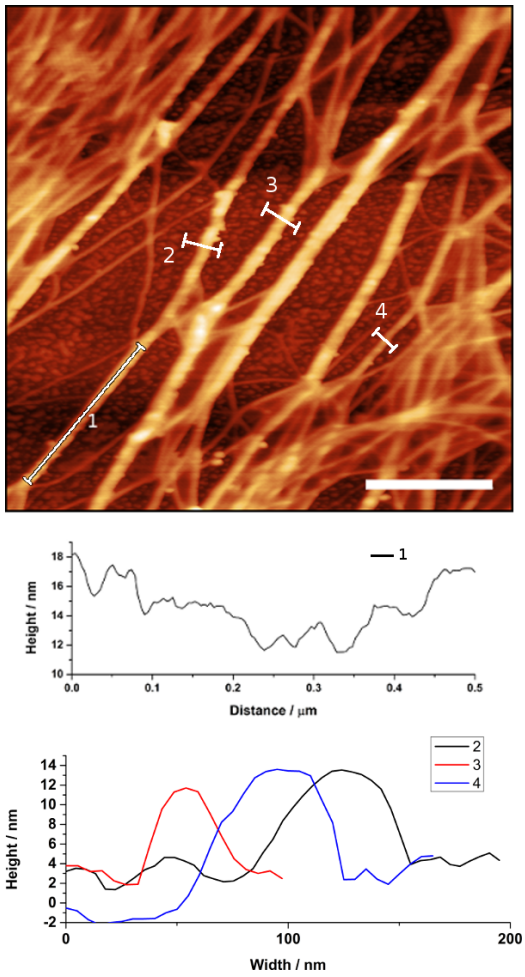

Figure S6. –Tapping-mode AFM (TM-AFM) image of undoped EB TANI-PTAB forming fibres on an HOPG substrate (upper image), with line profile of marked sections below (lower images) Scale bar: 500 nm

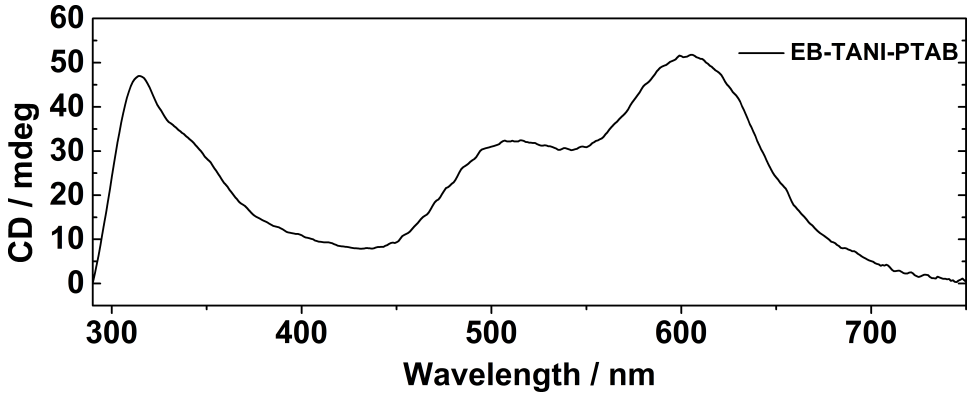

Figure S7. CD spectrum of EB TANI-PTAB (4 mM, aqueous). Observed signal closely resembles the UV-Vis spectrum of EB TANI-PTAB, and is suggested to arise from macroscopic sample alignment[1] that was inadvertently induced during filling of the narrow pathlength cuvette required to study the very highly absorbing solution and obtain reliable data. No bisignate features occur for the EB state material.

Computational chemistry: DFT modelling of EB TANI-PTAB

Computational details

Calculations which accurately capture the structural and electronic properties of aniline oligomers remain a significant challenge,[2] and were undertaken here to aid the interpretation of experimentally observed properties, focusing on only the simpler emeraldine base (EB) oxidation state of TANI, which has been treated by similar methods previously.[3] The doped species, TANI(CSA)$_2$-PTAB, was not considered, as the modelling of charged radical species with associated anions poses additional computational challenges, outside the scope of the present work. Calculations were performed to support the assignments of experimentally observed UV-Vis transitions, and to predict the orientation of the associated transition dipole moments, for EB TANI-PTAB. The geometry of EB TANI-PTAB was optimised using the B3LYP[4-7] functional with a standard 6-31G* basis set but with only the five spherical harmonic components of the polarization functions and a polarizable continuum model (PCM) solvation field[8,9] with water as solvent, as implemented in Gaussian 09, revision D.01.[10] Time-dependent DFT (TD-DFT) calculations with the CAM-B3LYP[11] functional (as suggested by Tozer et al.[12-14] for complexes with increased charge transfer character) were then used to calculate the excitation energies for the first 20 singlet transitions, using the B3LYP-optimised geometry as input. From these calculations the transition dipole moments were also extracted. Visualisation of the transition dipole moment in 3D space was accomplished using GabEdit[15] to overlay the (x, y, z) coordinates of the transitions as produced by TD-DFT calculations on the optimised Cartesian coordinates of TANI-PTAB.

The output of TD-DFT calculations for the first 10 excited states is detailed below, with images of the contributing molecular orbitals (MOs) (Figure S7). While one would expect the TD-DFT to capture well what is happening experimentally, i.e. several MOs of appropriate symmetry contributing to transitions to an excited state, it is worth noting that the standard (non-TD) B3LYP calculation gives a single point HOMO-LUMO gap in good agreement with experimentally observed transitions. This is no longer the case when performing a CAM-B3LYP single point calculation on the same geometry (Table 1). Additionally, CAM-B3LYP optimised geometries are generally in poorer agreement with available structural data (unpublished results). In contrast, TD-DFT calculations with CAM-B3LYP on the B3LYP optimised geometry give a closer match to the experimentally observed transition energies than do TD-DFT calculations with B3LYP, and this agrees with in-house benchmarking for different functionals (unpublished). We have therefore used this mixed method approach.

Method	Functional	HOMO-LUMO gap / eV (nm)	First excited state energy / eV (nm)
DFT geometry optimisation	B3LYP	2.1987 (563.9)	-
TD-DFT	B3LYP	2.1968 (564.4)	1.9562 (633.8)
TD-DFT	CAM-B3LYP	4.3532 (284.8)	2.4125 (513.9)

Table S1 - Comparison of DFT methodology showing calculated HOMO-LUMO and first excited state energies for relevant functionals

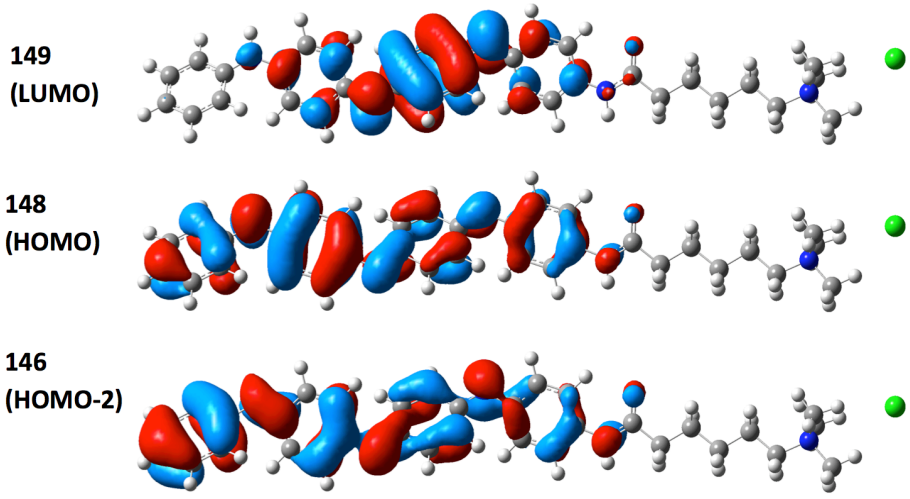

Figure S8 - MOs of EB TANI-PTAB contributing to the experimentally observed UV-Vis transition

Excited state energies:

Excited State 1: Singlet-A 2.4125 eV 513.93 nm f=1.4544
146 ->149 -0.10541
148 ->149 0.66460
Excited State 2: Singlet-A 2.9348 eV 422.47 nm f=0.0565
136 ->149 -0.11983
137 ->149 -0.19709
146 ->149 0.22149
147 ->149 0.60690
Excited State 3: Singlet-A 3.8962 eV 318.22 nm f=0.5479
135 ->149 0.37175
139 ->149 0.42229
141 ->149 0.22909
146 ->149 0.14486
147 ->149 -0.10267
148 ->149 0.17730
Excited State 4: Singlet-A 4.1481 eV 298.90 nm f=0.3304
137 ->149 -0.39701
139 ->149 -0.15936
140 ->149 0.12752
146 ->149 0.40281
147 ->149 -0.28945
Excited State 5: Singlet-A 4.2877 eV 289.16 nm f=0.0075
136 ->149 0.57000
137 ->149 -0.31356
140 ->149 0.14068
146 ->149 -0.14262
Excited State 6: Singlet-A 4.3887 eV 282.51 nm f=0.0052
136 ->149 -0.12007
137 ->149 0.10023
139 ->149 0.14617
140 ->149 0.41637
140 ->150 0.11398
141 ->149 -0.10367
147 ->151 0.10525
148 ->150 0.13761
148 ->151 -0.38693
148 ->153 0.18437
Excited State 7: Singlet-A 4.5412 eV 273.02 nm f=0.0007
136 ->149 -0.11732
139 ->149 -0.20166
140 ->149 0.15650
141 ->149 0.51972
141 ->150 -0.13411
147 ->152 -0.24193
147 ->155 0.10726
148 ->152 -0.15210
Excited State 8: Singlet-A 4.6844 eV 264.67 nm f=0.0933
140 ->149 -0.19801
147 ->151 0.10796
147 ->153 0.12808
148 ->150 0.51533
148 ->151 -0.18372
148 ->152 0.10118
148 ->153 -0.22511
Excited State 9: Singlet-A 4.7250 eV 262.40 nm f=0.0260
134 ->149 0.17773
136 ->149 0.29253
137 ->149 0.35957
139 ->149 -0.14244
146 ->149 0.40952
Excited State 10: Singlet-A 4.8465 eV 255.82 nm f=0.1047
139 ->149 0.10534
140 ->149 0.30965
146 ->154 0.15928
147 ->153 0.11022
147 ->154 -0.14621
148 ->150 0.13792
148 ->151 0.29223
148 ->153 -0.29449
148 ->154 0.30090

Table S2: Excited state energies and transitions calculated for EB TANI-PTAB

Transition dipole moment orientation

Orientation of calculated transition dipole moments (x, y, z coordinates):

State	X	Y	Z	Oscillator strength
1	4.9303	0.4021	0.3714	1.4544
2	0.8841	0.0545	0.036	0.0565
3	2.3759	0.3054	0.0341	0.5479
4	-1.7645	-0.3566	-0.1017	0.3304
5	0.2525	0.0681	0.0542	0.0075
6	0.1458	-0.1334	0.0979	0.0052
7	-0.0744	0.015	0.0271	0.0007
8	0.9004	0.0042	0.0517	0.0933
9	-0.3496	-0.2303	-0.2222	0.026
10	0.8412	0.2498	-0.3338	0.1047

Table S3: Calculated orientation and oscillator strength of transition dipole moments for EB TANI-PTAB

Coordinates of optimized geometry: EB TANI-PTAB

E =	-2089.575687	a.u.	
	X	Y	Z
C	-3.775695	1.663393	-0.625066
H	-3.704657	2.688456	-0.97717
C	-4.977734	1.060406	-0.47046
H	-5.887122	1.596573	-0.716426
C	-5.073128	-0.329559	-0.03018
C	-3.808502	-1.028069	0.177108
H	-3.880065	-2.05866	0.51279
C	-2.605617	-0.425079	0.029021
H	-1.694209	-0.966708	0.255235
C	-2.509971	0.971037	-0.393937
N	-6.162679	-1.02805	0.17536
N	-1.417601	1.668718	-0.569831
C	-7.446266	-0.50297	0.21703
C	-10.170602	0.326361	0.345624
C	-8.497364	-1.337139	-0.226432
C	-7.805783	0.751922	0.766296
C	-9.131983	1.147152	0.838322
C	-9.821912	-0.928571	-0.199247
H	-8.241253	-2.310213	-0.635052
H	-7.043028	1.391717	1.197657
H	-9.382868	2.100248	1.2973
H	-10.586855	-1.577527	-0.608523
C	-0.136513	1.116617	-0.557025
C	2.549885	0.20659	-0.564089
C	0.226449	-0.070567	-1.229762
C	0.891152	1.851525	0.06789
C	2.206751	1.403064	0.092044
C	1.544478	-0.50898	-1.237407
H	-0.522069	-0.627729	-1.783952
H	0.631612	2.783979	0.560731
H	2.97323	1.97106	0.599213
H	1.800452	-1.418362	-1.776161
N	3.856572	-0.317751	-0.605683
N	-11.471862	0.807667	0.400738
H	3.948507	-1.187599	-1.115654
H	-11.553768	1.810076	0.511146
C	-12.690278	0.122405	0.280088
C	-15.20934	-1.126913	0.076487
C	-13.809463	0.833724	-0.192024
C	-12.854237	-1.219815	0.667198
C	-14.102545	-1.833262	0.553075
C	-15.053971	0.214866	-0.285232
H	-13.693114	1.873197	-0.488883
H	-12.019626	-1.773184	1.082102
H	-14.208878	-2.871188	0.857298
H	-15.904132	0.783962	-0.651677
H	-16.177953	-1.610973	-0.005734
O	5.060948	1.195389	0.634152
C	5.005414	0.152437	-0.014477
C	6.214534	-0.760963	-0.207804
H	6.139321	-1.564398	0.539859
H	6.162853	-1.251381	-1.188058
C	7.547778	-0.02539	-0.044533
H	7.551555	0.494095	0.92022
H	7.633422	0.750952	-0.816071
C	8.748698	-0.975208	-0.132214
H	8.654213	-1.755469	0.635544
H	8.742659	-1.490005	-1.102784
C	10.088216	-0.239863	0.048669
H	10.086183	0.267838	1.019495
H	10.179635	0.530261	-0.725029
C	11.243158	-1.235119	-0.040346
H	11.145666	-2.006144	0.728526
H	11.24921	-1.727938	-1.01614
N	12.645441	-0.659801	0.13365
Cl	16.382278	0.670642	0.563792
C	13.637288	-1.787635	-0.01514
H	14.63885	-1.37286	0.117498
H	13.424702	-2.540124	0.745274
H	13.525425	-2.219454	-1.010464
C	12.826405	-0.048279	1.499481
H	13.866084	0.276664	1.579172
H	12.596768	-0.803735	2.252147
H	12.154699	0.802536	1.603179
C	12.94917	0.378941	-0.915084
H	12.787173	-0.06306	-1.899235
H	12.28957	1.233687	-0.773315
H	13.99155	0.679544	-0.788615

Table S4: Atomic coordinates for calculated ground state model of EB TANI-PTAB, and corresponding calculated ground-state energy of the structure.

References

(1) Wolffs, M.; George, S. J.; Tomović, Ž.; Meskers, S. C. J.; Schenning, A. P. H. J.; Meijer, E.W. *Angew. Chemie, Int. Ed.* **2007**, *119*, 8351–8353.

(2) Udeh, C. U.; Fey, N.; Faul, C. F. J. *J. Mater. Chem.* **2011**, *21*, 18137–18153.

(3) Shao, Z.; Rannou, P.; Sadki, S.; Fey, N.; Lindsay, D. M.; Faul, C. F. J. *Chem. - A Eur. J.* **2011**, *17*, 12512–12521.

(4) Becke, A. D. *J. Chem. Phys.* **1993**, *98*, 5648.

(5) Lee, C.; Yang, W.; Parr, R. G. *Phys. Rev. B* **1988**, *37*, 785–789.

(6) Vosko, S. H.; Wilk, L.; Nusair, M. *Can. J. Phys.* **1980**, *58*, 1200–1211.

(7) Stephens, P. J.; Devlin, F. J.; Chabalowski, C. F.; Frisch, M. J. *J. Phys. Chem.* **1994**, *98*, 11623–11627.

(8) Miertuš, S.; Scrocco, E.; Tomasi, J. *Chem. Phys.* **1981**, *55*, 117–129.

(9) Pascual-ahuir, J. L.; Silla, E.; Tuñon, I. *J. Comput. Chem.* **1994**, *15*, 1127–1138.

(10) Frisch, M. J. T.; Rucks, G. W.; Schlegel, H. B.; Scuseria, G. E.; Robb, M. A.; Cheeseman, J. R.; Scalmani, G.; Barone, V.; Mennucci, B.; Petersson, G. A.; Nakatsuji, H.; Caricato, M.; Li, X.; Hratchian, H. P.; Izmaylov, A. F.; Bloino, J.; Zheng, G.; Sonnenberg, J. L.; Hada, M.; Ehara, M.; Toyota, K.; Fukuda, R.; Hasegawa, J.; Ishida, M.; Nakajima, T.; Honda, Y.; Kitao, O.; Nakai, H.; Vreven, T.; Montgomery, J. A. J.; Peralta, J. E.; Ogliaro, F.; Bearpark, M.; Heyd, J. J.; Brothers, E.; Kudin, K. N.; Staroverov, V. N.; Kobayashi, R.; Normand, J.; Raghavachari, K.; Rendell, A.; Burant, J. C.; Iyengar, S. S.; Tomasi, J.; Cossi, M.; Rega, N.; Millam, J. M.; Klene, M.; Knox, J. E.; Cross, J. B.; Bakken, V.; Adamo, C.; Jaramillo, J.; Gomperts, R.; Stratmann, R. E.; Yazyev, O.; Austin, A. J.; Cammi, R.; Pomelli, C.; Ochterski, J. W.; Martin, R. L.; Morokuma, K.; Zakrzewski, V. G.; Voth, G. A.; Salvador, P.; Dannenberg, J. J.; Dapprich, S.; Daniels, A. D.; Farkas, Ö.; Foresman, J. B.; Ortiz, J. V.; Cioslowski, J.; Fox, D. J. Gaussian 09, 2009, Wallingford CT.

(11) Yanai, T.; Tew, D. P.; Handy, N. C. *Chem. Phys. Lett.* **2004**, *393*, 51–57.

(12) Peach, M. J. G.; Helgaker, T.; Sałek, P.; Keal, T. W.; Lutnaes, O. B.; Tozer, D. J.; Handy, N. C. *Phys. Chem. Chem. Phys.* **2006**, *8*, 558–562.

(13) Peach, M. J. G.; Benfield, P.; Helgaker, T.; Tozer, D. J. *J. Chem. Phys.* **2008**, *128*, 044118.

(14) Wiggins, P.; Williams, J. A. G.; Tozer, D. J. *J. Chem. Phys.* **2009**, *131*, 091101.

(15) Allouche, A. R. *J. Comput. Chem.* **2011**, *32*, 174–182.